

**Title:**

Insights into the Materials and Technique of a Roman Egyptian Funerary Portrait Obtained from Elemental Mapping and Luminescence Imaging

**Author(s):**

Stephanie Spence and John Twilley

**URL:**

<http://localhost:8080/14/>

**Citation:**

Spence, Stephanie, and John Twilley. "14. Insights into the Materials and Technique of a Roman Egyptian Funerary Portrait Obtained from Elemental Mapping and Luminescence Imaging." In *Mummy Portraits of Roman Egypt, Volume 2: Emerging Research from the APPEAR Project*, by Caroline R. Cartwright and Marie Svoboda. Los Angeles: J. Paul Getty Museum, 2026. <http://localhost:8080/14/>.

© 2026 J. Paul Getty Trust

The text of this work is licensed under a Creative Commons Attribution-NonCommercial 4.0 International License. All images are reproduced with the permission of the rights holders acknowledged in the captions and are expressly excluded from the CC BY-NC license covering the rest of this publication. These images may not be reproduced, copied, transmitted, or manipulated without consent from the owners, who reserve all rights. To view a copy of this license, visit <https://creativecommons.org/licenses/by-nc/4.0/>.

Getty

# Insights into the Materials and Technique of a Roman Egyptian Funerary Portrait Obtained from Elemental Mapping and Luminescence Imaging

*Stephanie Spence  
John Twilley*

The collection of the Nelson-Atkins Museum of Art contains a Roman Egyptian funerary portrait from Antinoöpolis stylistically dated to the second century CE. Acquired in 1937, this encaustic painting on wood panel is representative of a corpus of funerary portraits painted during the Roman rule of Egypt from the first through third centuries CE. The portrait depicts a young woman with an austere expression, dressed in a deep red tunic with a black-and-white striped collar (or undertunic), and black clavi at the shoulders (fig. 14.1). The sitter is set against a dark gray background that transitions to a light gray highlight directly behind her head. The woman's large, almond-shaped eyes are accentuated by individually painted lashes, and thick, arched eyebrows. Deep shadows and bright highlights on her olive complexion emphasize her strong features. Her jewelry, rendered in relief using gilt stucco, includes pendant earrings in the form of grape clusters, a gold necklace inset with dark blue stones modeled in painted stucco, and two hairpins that secure hair piled tightly atop her head in a thick plait. Multiple

application techniques can be observed, including the marks of a sharp, pointed instrument used to render complex shading and delicate details of the face, neck, and head, while wide, vertical brushstrokes were used in the garment and background.

One gilt stucco hairpin and the right earring are lost, revealing the wood support and stucco remnants. The necklace's painted blue stones are darkened by accretions and dirt that visually obscure the original color. The painted surface of the stone located to the proper left of the central stone is lost, leaving behind broken stucco remnants. The central blue stone in the necklace is cracked down its center, correlating to the vertical split through the center of the wood panel that was mended prior to painting and repaired by modern intervention. A clear coating applied along the central split below the large loss in the woman's hair has darkened the paint surface from the forehead to the right nostril. The paint surface near the

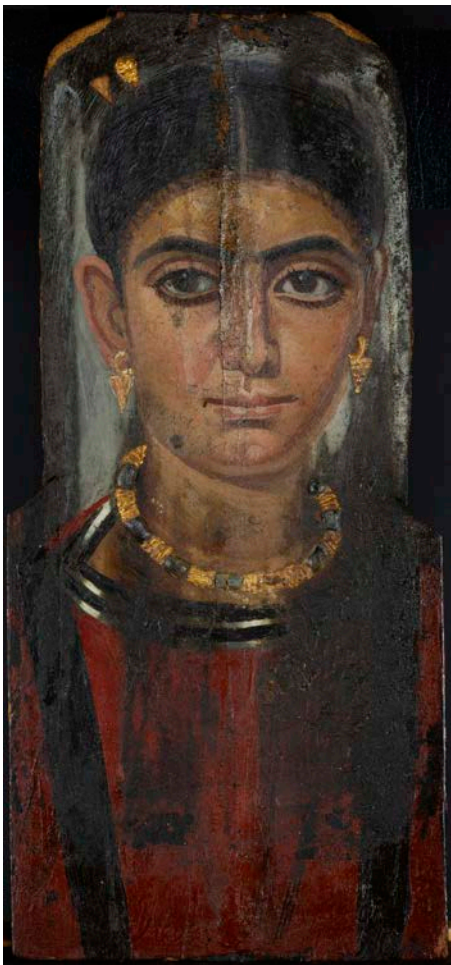


**Figure 14.1** Portrait of a Woman, Romano-Egyptian, ca. 131–160 CE. Encaustic on wooden panel with gilt stucco, 44.5 x 17 cm (17 1/2 x 6 3/4 inches); panel thickness: 4 mm. Kansas City, the Nelson-Atkins Museum of Art, 37-40. Photo: S. Spence and K. Hamilton, Courtesy of the Nelson-Atkins Museum of Art

bottom of the panel is slightly sticky, with dust fibers stuck to the surface.

There are cracks in the encaustic surface throughout the portrait. The most significant paint losses are located at the top of the panel around the central crack and throughout the garment. Blanching of the paint surface has occurred in the dark background, namely along the proper left side, in smaller portions of the hair, and along the upper proper right side. Black surface deposits and staining visibly obscure a large portion of the sitter's garment and extend into the neck. The paint surface hidden below these accretions on the proper left side is damaged with some paint loss. The paint is smeared around the collar and tunic, suggesting the wax was in a softened state when this damage occurred. The black deposits terminate around the outer edges of the clavi, several inches above the bottom of the panel, suggesting

the outer edges of the panel were somehow protected from these deposits. Although there is no visual evidence of textile on the front, the well-preserved edges may indicate where the linen wrappings once secured the panel in place over the head of the mummified remains.

All that is known of the painting's provenience is based on art historical critique from visual examination. The shape of the Nelson-Atkins panel, which lacks all outer remnants of the mummy wrappings, exhibits stepped shoulders that have been recognized as a unique characteristic of works from Antinoöpolis.<sup>1</sup> Portraits from Antinoöpolis are cited for the depiction of solemn subjects wearing austere fashion, tightly confined hair styles, and include women often swathed in drapery.<sup>2</sup> Scholars have narrowly attributed the portrait to the early Antonine period (131–160 CE) based on her hairstyle, which is parted down the center and piled atop her head in a thick bun with a line of fine curls at the forehead.<sup>3</sup>

This paper focuses on a recent technical study that attempted to broaden our understanding of this encaustic work by clarifying the artist's working techniques and material choices not accessible through visual assessment alone. As more portraits are added to the Getty's APPEAR (Ancient Panel Paintings: Examination, Analysis, and Research) project database, comparison of the Nelson-Atkins's single example of this type of portrait with those from other collections may contribute to a better understanding of the group.

## METHODS

Several non-sampling examination techniques were employed to investigate the materials, composition, and working techniques of the portrait, followed by microanalyses of a small number of samples. The structure, condition, and extent of restoration were investigated without sampling by X-radiography, multiband imaging (MBI), and surface microscopy. MBI employs technology to observe an object in wavelength ranges that extend beyond the capabilities of the human eye, from the ultraviolet (UV) to the near infrared (NIR).<sup>4</sup> Images were captured using a UV-VIS-IR-modified Nikon D7000 DSLR camera with a 60mm lens and a set of UV-VIS-IR bandpass filters. While the imaging set was comprehensive, only those images with diagnostic relevance will be discussed.

Elemental mapping by X-ray fluorescence spectrometry (XRF) was conducted on the painting using a small, portable instrument built in-house following a design provided by collaborators from the Laboratoire

d'archéologie moléculaire et structurale–Centre national de la recherche scientifique (LAMS-CNRS), Paris, that has been previously published.<sup>5</sup> Our instrument differs from the published design only in its use of a machined aluminum coupling component that offers improved heat dissipation for the detector's electronics and two-axis motion in only X and Y directions. The essential features and operating conditions of the instrument include a Moxtek end-window X-ray tube with Pd anode, operated at 40kV and 50 $\mu$ A, and an Amptek X123 SDD detector with 25mm<sup>2</sup> area. The tube output is collimated by a 0.7mm diameter Pd tube yielding an effective spot size of 1mm at the standoff distance of 15mm. Maps were acquired in two rectangular runs overlapping in the region where the panel width increases, one for the face and the other for the torso. The face was acquired over a 170 x 240mm area at 1mm spacings using dynamic acquisition (on the fly) with an acquisition interval of 0.5 seconds per spectrum. The torso acquisition was done over 205 x 210mm with a longer dwell time of 0.75 seconds. Acquisition control was programmed in Python and spectra were fitted using PyMca.<sup>6</sup> Elemental maps output with 32-bit grayscale were rescaled to 8-bits for reproduction as standard graphics.

Microsamples from the red tunic and hazy background deposits were analyzed by polarized light microscopy (PLM) and scanning electron microscopy coupled with energy-dispersive X-ray spectrometry (SEM-EDX).

## RESULTS AND DISCUSSION

### *Egyptian Blue*

Egyptian blue, the synthetic blue pigment composed of copper calcium silicate, exhibits unique and intense photoluminescence that provides a complementary method to reflectance spectroscopy. The strong photo-induced near-infrared (NIR) luminescence emission at 910nm has been used as a characteristic marker to identify and map Egyptian blue in ancient paintings using visible-induced infrared luminescence (VIL) photography.<sup>7</sup>

Egyptian blue was initially discovered in the painting with VIL, showing sharply defined strokes contouring the figure's eyes, brow line, head, and neck (fig. 14.2). XRF elemental mapping showed copper concentrations in the same areas of the face and neck, confirming the use of Egyptian blue in the painting (fig. 14.3A) while also disclosing copper in another form in the dark blue stones of the necklace. The stones are rendered in stucco relief and painted with a second copper-containing pigment that has not been identified in this study. Although the painting

does not appear to visually employ Egyptian blue in the facial features, VIL and XRF uncovered the artist's use of the blue pigment in two distinct roles: (1) as a means of sketching the underdrawing and (2) in the modulations of flesh tones in the upper-layer stratigraphy.



**Figure 14.2** VIL image showing the presence of Egyptian blue in the face and neck of the portrait in figure 14.1. Camera: Nikon D7000 DSLR (modified), X-Nite 830nm filter. Lighting: ADJ LED panels in red light setting- CL01. Photo: S. Spence and K. Hamilton, Courtesy of the Nelson-Atkins Museum of Art

The copper response in the facial areas does not consistently correspond to either highlights or shadows but also seems to have been a means of laying out the proportions of the face as an underdrawing. A noticeable feature of the Egyptian blue distribution is the peak in each brow line that, together, form an "M." An X-radiograph of the portrait shows the density associated with the heavier Egyptian blue applications that appear to be sketch lines above the eyes and along the nose (fig. 14.4). While lead white is also present in the face and contributes to the total radiographic density, the Egyptian blue application correlates to locations of increased density in the radiograph. When comparing the VIL image and copper map to the visible light image, the lines of Egyptian blue are in close proximity to the highlight above the eyebrows containing lead. Several blue particles are visible on the surface of the highlights when viewed under magnification, indicating the presence of some Egyptian blue in the paint mixture. A direct overlay of the elemental maps for copper and lead shows, however, some offset of the areas of maximum intensity for the two elements in the eyebrow and nose constructions. The lines for Egyptian

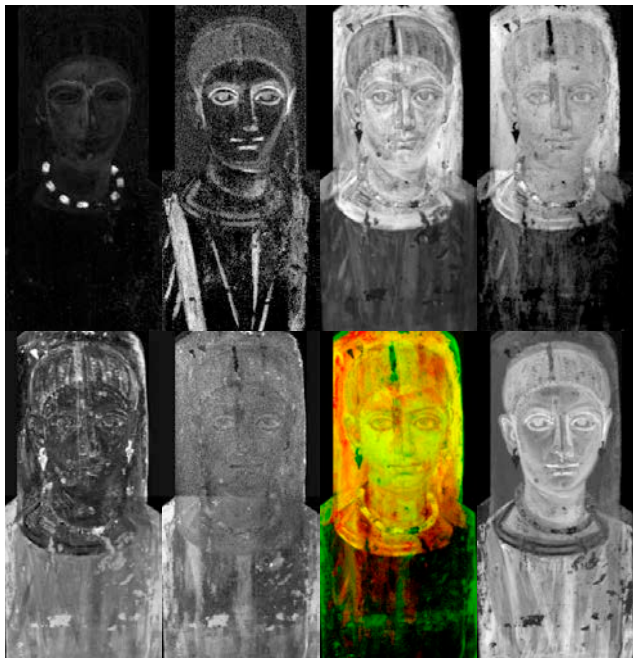


**Figure 14.3** (A) Copper distribution map derived from XRF elemental mapping corroborates the Egyptian blue found in the same areas of the VIL image in figure 14.2. Higher copper concentrations in the three-dimensional necklace beads indicate that a different copper-based pigment was used there. (B) Manganese distribution map derived from XRF elemental mapping demonstrating a pronounced difference in manganese content between the two dark vertical stripes that reveals the artist's adjustment of the pigment mixture in accordance with the illumination direction. (C) Lead distribution map based on the Pb L-lines shows the selective use of lead pigment in the upper portion of the panel. (D) Lead distribution map based on the lower energy Pb M-lines also corroborates the selective application of lead in the portrait. (E) Calcium distribution map showing the muted response of calcium in much of the upper portion of the panel where Ca emissions from the preparation layer are absorbed by overlying lead paint. (F) The sulfur distribution map also shows a muted response in the upper region, suggesting that the presence of both S and Ca is indicative of a gypsum layer applied below the upper paint layers containing Pb. (G) False-color RGB image in which Pb M-lines and Cl K-lines have been assigned to the red and green channels, respectively. The resulting yellow color is indicative of the correlation of these two elements and corresponds closely to the distribution of haze formations around the head. (H) Iron map demonstrating the important role of iron pigments throughout the composition. Photos: J. Twilley, Courtesy of the Nelson-Atkins Museum of Art

blue fall slightly below and to the left of surface highlights that correspond to the lead map above the eyebrows and along the nose, respectively.

Underdrawings detected in a small number of portraits to date have more often relied on carbon black or madder than on Egyptian blue.<sup>8</sup> The prominent role of Egyptian blue in this painting and its use in sketchwork are not apparent in normal viewing. In the absence of historical accounts of artists' techniques from the period, a possible explanation could be that the pigment's coarse texture allowed the sketch to remain perceptible beneath successive paint applications as an increased roughness



**Figure 14.4** X-radiograph revealing greater radio-opacity associated with the M-shaped lines of Egyptian blue seen in the VIL image (fig. 14.2) and the greater thicknesses of the relief decorations, including those visible in the Cu distribution map (fig. 14.3A). Settings: 60kV; 3mA; 5 second exposure; film. Photo: J. Rogers, Courtesy of the Nelson-Atkins Museum of Art

until the work was nearly complete. A portrait of a woman excavated from the site of Tebtunis in the collection of the Phoebe A. Hearst Museum of Anthropology (PAHMA #6-21375) shows another example of Egyptian blue identified in the face that appears to be employed as an underdrawing, also discovered through VIL and complementary XRF methods.<sup>9</sup> Much like that of the Nelson-Atkins's sitter, VIL reveals Egyptian blue in outlines along her face and on the "M" above the sitter's eyebrows.

The more common role of Egyptian blue—mixed with other pigments to enhance their colors<sup>10</sup>—is also seen in the Nelson-Atkins's portrait. Egyptian blue was used to modulate flesh tones in both highlights and shading around the eyes, ears, nose, neck, and forehead. While a blue hue is imperceptible in these areas, examination of the paint surface under a stereomicroscope revealed particles of Egyptian blue in corresponding areas of highlights and shading as suggested in the VIL image and copper distribution map (fig. 14.5). Along with unproven examples, portraits from Hawara and Saqqara have been found to utilize Egyptian blue in this manner.<sup>11</sup> A VIL study of Egyptian blue in Roman Egyptian funerary portraits from the Cantor Arts Center at Stanford University<sup>12</sup> confirmed the pigment was used in idiosyncratic ways in the flesh tones, garments, and eyes, but its use for underdrawing is noticeably absent from those findings.



**Figure 14.5** Photomicrograph showing blue particles visible in the paint surface of the highlight under the sitter's right eye, corresponding to the regions with VIL responses for Egyptian blue (fig. 14.2) and XRF responses for copper (fig. 14.3A), as seen in the stereobinocular microscope with fiber optic illumination. Photo: S. Spence, Courtesy of the Nelson-Atkins Museum of Art

## Umber

Elevated levels of manganese in dark areas of the painting were identified with elemental mapping. Manganese is elevated in shadows of the garment folds and shading of the facial features, both presumably using some form of umber (fig. 14.3B). Umber is known to be used in varying proportions with iron-earth pigments, carbon black, and lead white to achieve variations in brown tones in mummy portraits.<sup>13</sup> A reflected infrared (IRR) image serves to differentiate nuances in dark brown and black passages when compared to the distribution of manganese derived from XRF mapping by revealing the distribution of carbon blacks not detectable with XRF (fig. 14.6). The IRR image demonstrates that carbon black was utilized in areas such as the hair, eyes, eyebrows, clavi, striped collar, and dark shading in the tunic.

It is clear from this comparison that manganese and carbon black play distinct roles in the depiction of dark details in the portrait. The hair is painted overall with carbon black, iron, and a small amount of manganese. The central "V" folds and the drapery on the proper right sleeve rely heavily on manganese and very little carbon black, while the clavi on the garment are treated differently on the right and left. The proper right clavus contains more manganese than the proper left, even though the two seem to contain equivalent applications of carbon black, as evidenced by IRR. This differing treatment of the garment's symmetrical components could have contributed to a more naturalistic depiction, with illumination falling from the sitter's right side, and may

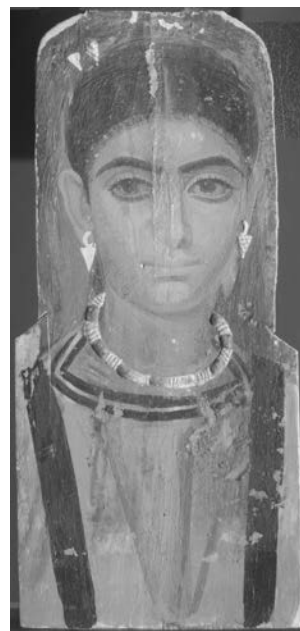


**Figure 14.6** IRR image in which light absorption by carbon black is the predominant feature, providing a useful comparison for the distribution of carbon black with that of umber pigments mapped by XRF. Camera: Nikon D7000 DSLR (modified), Kodak 87C filter. Lighting: Minipro LEE Colortran tungsten light. Photo: S. Spence and K. Hamilton, Courtesy of the Nelson-Atkins Museum of Art

have once been more evident than it is today in its stained state.

## Lead White

XRF mapping shows the presence of lead pigment in paint mixtures and its selective application to the region above the shoulders, including the gray background around the head, but it is noticeably absent from the torso (figs. 14.3C and D). The X-radiograph shows surprisingly little difference in density between the lead-containing background behind the head and the torso (see fig. 14.4). While this contrast is controlled by conditions of their radiography, the low contrast between the upper region and torso suggests that the lead pigment application is a thin one.

Comparison of the lead maps to XRF maps for calcium and sulfur helped to suggest the order of application of ground layers (figs. 14.3E and F). The distribution of calcium in the portrait is primarily indicative of the ground layer. The calcium map demonstrates that the heavier pigments in the upper part of the panel, such as lead, suppress the response from the relatively weaker calcium X-rays. In contrast, calcium X-rays are evident in the lower panel, especially in areas of paint loss and in the areas where the stucco earring and hairpin are missing in the upper panel.

From these findings, a calcium-based preparatory layer can be presumed to lie beneath the lead pigment on the upper panel.

The sulfur map further distinguishes the calcium-based preparatory layer identified above. With the XRF mapping apparatus employed in this study, the distribution of sulfur can be well differentiated from the overlapping response for lead M-lines, allowing calcium associated with sulfur in the form of one of the gypsum minerals to be distinguishable. This leads us to believe that a calcium sulphate ground layer was applied underneath the lead white. Additionally, this ability to separately resolve sulfur from the overlapping low-energy lead peak allows the lead response from the upper surface to be differentiated from that arising deeper in the paint layer, allowing for the comparison of the roles of lead pigment in different regions.

### Lead Chloride Formation

Irregular white hazy patches obscure the darker passages of the gray background toward the outer edges of the panel (fig. 14.7). The blanching is heavily concentrated along the background behind the sitter's proper left, with some encrustations partially covering the left ear and hairline. Additional areas of blanching are present at the crown of the head and to the proper right of the hairpins. Under magnification, much of the blanching appears as a superficial crust comprised of fine, yellowish white grains of varying sizes (fig. 14.8).

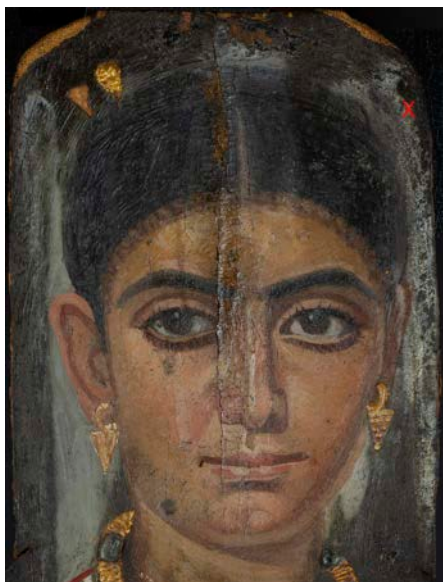


Figure 14.7 Reference image for the location (X) of the photomicrograph in figure 14.8. Photo: S. Spence, Courtesy of the Nelson-Atkins Museum of Art

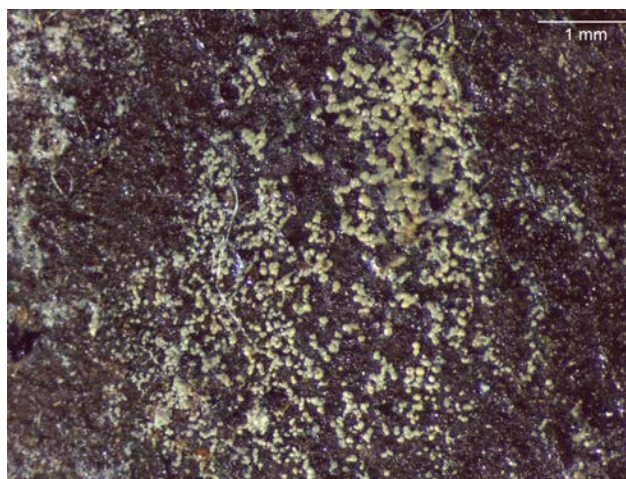


Figure 14.8 Photomicrograph of the Pb-Cl-rich white crust that has formed on the upper proper left side of the paint surface as seen in the stereobinocular microscope using fiber optic illumination. This detail shows the formation of individual yellowish white granules of varying size that appear to sit on top of the paint surface. Photo: S. Spence, Courtesy of the Nelson-Atkins Museum of Art

The element chlorine is also readily mappable with this XRF apparatus and appears to explain the blanched appearance of parts of the painting where its distribution follows that of the lead at the surface (fig. 14.3G). High levels of chlorine are visible along the proper left edge of the panel, coinciding with the heaviest concentration of the crust in the background. A microsample of this white material from the surface of the proper left side of the black background, adjacent to the sitter's hair, was further analyzed by SEM-EDX and found to consist of lead chloride without other detectable elements. This encrusted matter contained some beeswax medium identified by Fourier-transform infrared spectroscopy (FTIR) and had a gummy consistency. Unaltered lead pigment, when present in the sample, was distinguished by a finer particle size and lack of chloride. The implication of these white formations is that chloride salt, nearly ubiquitous in Egyptian artifacts from various sources and often derived from groundwater salinity or the burial environment, has interacted with the lead pigment to form lead chloride on the paint surface. Lead chloride is insoluble and thus favored to form in the interaction of most lead pigments with sodium chloride. This is a well-known phenomenon impacting not only wall paintings, but also easel paintings and lead-based architectural paints on masonry surfaces containing chlorides.<sup>14</sup>

A cross section from the forehead of a Tebtunis portrait (#6-21378b) in the PAHMA collection also contained a lead chloride compound as the main constituent in a white crust layer.<sup>15</sup> A specific identification of the crust-forming

compound as  $\text{KPb}_2\text{Cl}_5$  was obtained in that case by synchrotron-based micro X-ray diffraction mapping of the cross section. Therefore, while the two cases are closely related, the end product is different.

### ***Iron-Based Pigments Including Red Ochre***

The map for iron shows the extensive use of iron earths in the artist's palette (fig. 14.3H). Virtually every component of the composition relies upon iron in some form, including the red garment, all of the skin tones, and even the black in the hair. The overall red of the garment as well as its folds are rendered as variations in the distribution of this element. The rounding of the facial features in the later stages of painting that contrasts with their angularity in the Egyptian blue underdrawing is exemplified by their shapes in the iron map. The iron map also resolves pigment strokes in the hair more clearly than any other single element. It discloses the texture of the hair that could be interpreted as rows of braids at the front of the head, as well as a distinct boundary between the volume of the top of the head and that of the tightly braided hair bun in the back.

The depth of the tunic's red color suggested that this area might make use of organic lake pigment in addition to the iron-based pigment found there with elemental mapping. Ultraviolet-induced visible fluorescence (UVF) imaging showed, however, no evidence of the distinctive pink/orange fluorescence of lake pigments, such as madder (fig. 14.9). The irregular, dull orange fluorescence visible with UVF in much of the red garment also extends into most areas of the portrait, with the exception of the face. A thin strip of the red tunic and striped collar next to the inner edge of the proper right clavus is also devoid of this orange fluorescence. It is more likely that this fluorescence corresponds to a clear surface coating that was not identified in this study. The tunic also appears dark in the false-color ultraviolet (FCUV) image, corroborating the presence of red ochre without the addition of a lake pigment (fig. 14.10).<sup>16</sup>

A microsample from the red tunic near the bottom edge of the panel was examined by polarized light microscopy (PLM) and SEM-EDX to determine whether the inorganic elements detected in the garment fully accounted for its red color. PLM shows that the sample only contains a dilute amount of very fine red iron oxide particles that have been well dispersed in an excess of wax medium, causing it to function like a colored varnish and deepening its color by reducing light scattering from the surface (fig. 14.11). It is not known if red lead has been incorporated into the painting's composition elsewhere, but the lead



**Figure 14.9** The UVF image does not show a response attributable to any lake pigments in the red tunic, but does show areas of restoration in the portrait, particularly down the center of the face, that correspond to the split in the wood panel. Camera: Nikon D7000 DSLR (modified), BG38 + PECA 918 + Kodak 2E filters. Lighting: Wildfire Viostorm VS-60 with a visible-cut filter. Photo: S. Spence and K. Hamilton, Courtesy of the Nelson-Atkins Museum of Art



**Figure 14.10** The dark appearance of the red tunic in the FCUV image indicates the color is attributable to red ochre. This image was created through digital post-processing by combining visible and ultraviolet reflectance images. Photo: S. Spence and K. Hamilton, Courtesy of the Nelson-Atkins Museum of Art

map suggests a sparse presence of lead of unknown type in the upper regions of the red tunic (see figs. 14.3D and G). None was found in the PLM sample.

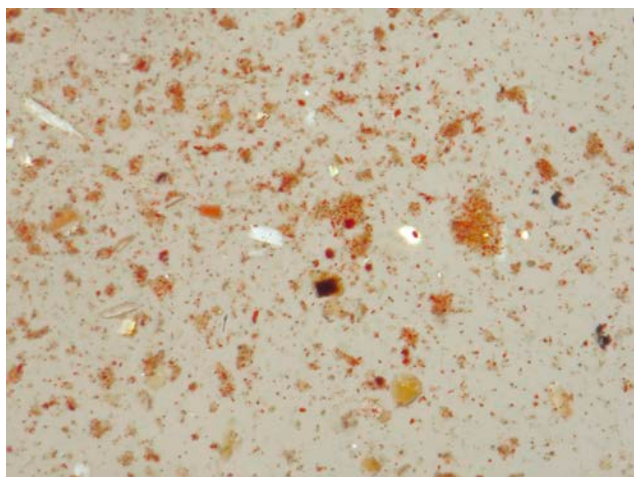


**Figure 14.11** Pigment particle dispersion from the bottom edge of the red tunic confirming the presence of very fine particles of red iron oxide dispersed in an excess of medium, partially crossed polars, 100x. Photo: J. Twilley, Courtesy of the Nelson-Atkins Museum of Art

## RESTORATIONS

A vertical split down the center of the panel shows evidence of both ancient and modern interventions. The paint has been consolidated in the worst areas of damage along the split in the head with a clear, glossy coating. UVF shows this coating has a milky, white fluorescence, but additional testing has not been carried out to identify it (see fig. 14.9). Due to the obvious presence of restoration coatings along the split, especially around the areas of paint loss in the head, it was assumed that repairs to the portrait occurred well after its completion, possibly at the time of excavation. However, no treatment documentation exists prior to or after its acquisition into the Nelson-Atkins collection.

The X-radiograph revealed further information about repairs to the lower half of the split hidden below the surface. While the split becomes invisible on the surface below the mouth, a narrow strip of plain-weave fabric beneath the paint layers was identified in the X-radiograph. Its texture becomes visible at the mouth and extends to the bottom of the panel (see fig. 14.4). The red tunic exhibits cracking that follows the fabric texture in some spots, but further disruptions to the paint surface that could indicate this textile was applied as a later repair, such as reworking of the wax or inpainting, are absent from the lower half of the portrait. Other splits in the panel

have not been bridged by fabric in this manner. The verso of the wood panel also has visible repairs along the crack. A dark brown resinous coating and sporadic patches of textile fragments are applied along the entirety of the vertical split (fig. 14.12). These textile fragments bear visual similarities to linen wrappings applied around funerary portraits when attached over the face of a mummy. This evidence suggests that the split in the panel was mended in preparation for painting.



**Figure 14.12** Repairs to the vertical split in the panel visible from the back include a dark, resinous fill material with six fabric patches applied along the break. The patches bear visual similarities to mummy wrappings used to attach funerary portraits atop the heads of mummified remains. Photo: S. Spence and K. Hamilton, Courtesy of the Nelson-Atkins Museum of Art

## CONCLUSIONS

From the time of its acquisition in 1937 until the undertaking of this technical study, the Nelson-Atkins's Roman Egyptian funerary portrait had been interpreted exclusively by means of art historical inquiry. Analysis by XRF elemental mapping and complementary imaging techniques, augmented by microanalytical techniques when necessary, has revealed hitherto unknown aspects of material usage and artist's practices. They reveal the use of Egyptian blue as an underdrawing, placing this painting within a larger corpus of funerary portraits that employed Egyptian blue as an additive to encaustic mixtures for flesh tones. The proportioning of carbon black and umber in the rendering of otherwise symmetrical dark passages of the painting reveal the painter's attempt to render the illumination of the sitter. The painter's choice of confining

the use of lead white to the upper half of the portrait is an unusual one for which no definitive explanation exists. The ability to map the distribution of chlorine by XRF demonstrated a correlation of this element with highly visible haze formations on the dark background. Confirmation of the alteration of lead white to lead chloride in SEM-EDX of haze samples, and the lack of chloride in paint not similarly affected, strongly suggests that exposure of this lead pigment to environmental chlorides over the lifetime of the portrait is the underlying cause of blanching of the dark passages behind the figure's head.

The analyses reported here have significantly furthered our understanding of the palette and working techniques in the Nelson-Atkins portrait. They have allowed us to explore both similarities and differences between this work and those investigated by other researchers, including some whose provenance is securely known. As a group, their working techniques are highly diverse and trends or groupings are only beginning to come into focus. Mineralogical analysis of the widely used earth pigments in the painting could advance our understanding of the individual pigments found in mixtures. The medium, which has not been investigated beyond FTIR confirmation that it is based upon beeswax, could provide further information about the painting through analysis by gas chromatography/mass spectrometry (GC/MS) methods. The wood and restoration materials remain yet to be identified as well. Future research of these materials will continue to broaden our knowledge of this portrait and its place within the history of Roman Egyptian funerary portraiture.

## ACKNOWLEDGMENTS

The authors would like to thank Kasey Hamilton for her contributions in imaging our portrait.

### NOTES

---

1. Doxiadis 1995; Parlasca 1966; Walker and Bierbrier 1997.
2. Walker and Bierbrier 1997.
3. Taggart 1959; Vermeule 1964; Doxiadis 1995.
4. Dyer and Newman 2020.
5. De Viguerie et al. 2018.
6. Solé et al. 2007.
7. Verri 2009A; Accorsi et al. 2009.
8. See Mahon et al., this volume; Mayberger et al. 2020.
9. Ganio et al. 2015.
10. Thiboutot 2020.
11. Dyer and Newman 2020; Park et al. 2019; Sabino et al. 2019.
12. Thiboutot 2020.
13. Park et al. 2019.
14. Ordonez and Twilley 1998.
15. Salvant et al. 2018.
16. Dyer and Newman 2020.